

# Blacklight: Defending Black-Box Adversarial Attacks on Deep Neural Networks

Huiying Li, Shawn Shan, Emily Wenger, Jiayun Zhang, Haitao Zheng, Ben Y. Zhao  
 Computer Science, University of Chicago  
 {huiyingli, shansixiong, ewillson, jiayunz, htzheng, ravenben}@cs.uchicago.edu

## Abstract

The vulnerability of deep neural networks (DNNs) to adversarial examples is well documented. Under the strong white-box threat model, where attackers have full access to DNN internals, recent work has produced continual advancements in defenses, often followed by more powerful attacks that break them. Meanwhile, research on the more realistic black-box threat model has focused almost entirely on reducing the query-cost of attacks, making them increasingly practical for ML models already deployed today.

This paper proposes and evaluates *Blacklight*, a new defense against black-box adversarial attacks. Blacklight targets a key property of black-box attacks: to compute adversarial examples, they produce sequences of highly similar images while trying to minimize the distance from some initial benign input. To detect an attack, Blacklight computes for each query image a compact set of one-way hash values that form a probabilistic fingerprint. Variants of an image produce nearly identical fingerprints, and fingerprint generation is robust against manipulation. We evaluate Blacklight on 5 state-of-the-art black-box attacks, across a variety of models and classification tasks. While the most efficient attacks take thousands or tens of thousands of queries to complete, Blacklight identifies them all, often after only a handful of queries. Blacklight is also robust against several powerful countermeasures, including an optimal black-box attack that approximates white-box attacks in efficiency. Finally, Blacklight significantly outperforms the only known alternative in both detection coverage of attack queries and resistance against persistent attackers.

## 1 Introduction

The vulnerability of deep neural networks to a variety of adversarial examples is well documented. Adversarial examples are maliciously modified inputs that not only produce misclassifications by a model, but also are nearly identical to original inputs via human perception. This vulnerability remains a critical hurdle to the practical deployment of deep learning systems in safety- and mission-critical applications, such as autonomous vehicles, financial services, or digital health services.

Adversarial attacks can be divided by whether they assume *white-box* or *black-box* threat models. In the white-box setting, the attacker has total access to the target model, including

its architecture and specific weights and parameters. Given a benign input, the attacker can compute adversarial examples as an optimization algorithm. In the black-box setting, the attacker is restricted from interacting with the model via queries and classification outputs. Black-box scenarios can be further divided into *score-* or *decision-based*, depending on whether the target model returns a full probability distribution across labels per query, or only the output label.

Under the strong white box threat model, both security and ML communities have made continual advances in both attacks and defenses. Powerful attacks provide more efficient and versatile algorithms to generate adversarial examples [9, 11, 18, 25, 50], which in turn spur work on robust defenses that either prevent the generation of adversarial examples or detect them at inference time. While numerous approaches have been explored as defenses, including model distillation [40], gradient obfuscation [5, 14, 31, 44, 47, 52], adversarial training [32, 55, 56], and ensemble methods [49], nearly all have been proven vulnerable to followup attacks [1, 6–8, 21].

In contrast, black-box attacks assume a more realistic threat model, where attackers interact with models via a query interface such as ML-as-a-service platforms [54], and do not require leaked models, server compromises or malicious insiders. One type of “substitute model” attacks uses black-box queries on the target model to train a substitute model, then tries to transfer adversarial examples from the substitute model to the target [29, 37, 38]. These can be effectively defended by training on adversarial examples built on pre-trained models [49]. More common attacks, however, are query-based attacks, where an attacker fine tunes the inputs based on query output from the target model, until they can converge upon an adversarial example with small perturbation from the original input. Multiple efforts have proposed increasingly efficient attack algorithms that continuously reduce the queries necessary for a successful attack against both score- and decision-based targets. Even as these attacks grow in efficiency and practicality, there are no published results describing effective defenses against them<sup>1</sup>.

In this paper, we propose *Blacklight*, a novel defense that detects query-based black-box attacks using an efficient simi-

<sup>1</sup>There is a defense described in an unpublished arxiv report [13], and we compare Blacklight against it in §7.

larity engine operating on probabilistic content fingerprints. Our detector relies on the fact that black-box attacks seek to generate adversarial examples whose perturbation from benign inputs is bounded. Thus the generation of an adversarial example requires the attacker to submit to the target model multiple queries that are similar to each other<sup>2</sup>. We detect this similarity across multiple queries as an attack, since this level of similarity rarely exists among benign queries.

Blacklight detects black-box attacks at inference time, by computing for each input query a probabilistic fingerprint composed of a small number of hash values. A query whose probabilistic fingerprint matches any prior fingerprint by more than a threshold is identified as part of a black-box attack. Fingerprint hashes are designed such that multiple inputs with small content differences will have high overlap in their fingerprint hashes. Since we use secure one-way hashes, even an attacker aware of our algorithm cannot optimize the perturbation to disrupt its fingerprints and avoid detection.

We evaluate the efficacy of Blacklight against 5 state-of-the-art query-based black-box attacks, including attacks using gradient estimation, gradient-free attacks, and attacks that target both score-based and decision-based models. We perform experiments over a range of image-based models from MNIST to ImageNet, and use  $L_p$  distance metrics chosen by each attack. Our results show that while these attacks typically take thousands (or tens of thousands) of queries to converge to a successful adversarial example, Blacklight detects these attacks after the first 2–6 queries<sup>3</sup>. Most importantly, Blacklight detects the large majority of all queries associated with an attack (>90% for all non-Boundary attacks), compared to <2% for the only other defense in literature [13]. For resource-rich attackers who persist after initial detection, Blacklight drops attack success rate to 0% (by rejecting each detected attack query), compared to 78%–100% when using [13].

In summary, our work makes five key contributions.

- We propose a highly scalable, lightweight detection system against query-based black-box attacks using probabilistic fingerprints.
- We use formal analysis of our probabilistic fingerprints to model both false positives and attack detection rates.
- We perform detailed experiments on multiple datasets and models to evaluate Blacklight against multiple state-of-art black-box attacks. Results show Blacklight can *quickly* detect attacks, often after a handful of queries for attacks that would require several thousands of queries to succeed.
- We compare Blacklight to the only known black-box defense [13], and it significantly outperforms in both queries detected and resistance against persistent attackers.

<sup>2</sup>In practice, even the most efficient black box attacks issue thousands of queries to generate a single attack, and nearly all such queries are constrained to be a small perturbation away from the benign input.

<sup>3</sup>The exception is the Boundary attack, which starts its query search with an image from the target label. Blacklight detects Boundary attacks after an average of less than 40 queries (see Table 5).

- Finally, we evaluate Blacklight and show that it is highly robust against a variety of adaptive countermeasures, including those allowing larger, human-visible perturbations. Blacklight performs well even against two types of *near-optimal* black-box attacks: “query-efficient” black-box attacks that are several orders of magnitude more efficient than current methods, and “perfect-gradient” black-box attacks that perfectly estimate the loss surface at each query, effectively approximating white-box attacks. Blacklight detects 100% of perfect-gradient black-box attacks that emulate CW (Carlini-Wagner), and 81% of those emulating PGD (projected gradient descent).

## 2 Background and Related Work

In contrast to early work on strong white-box attacks [9,26,35,39], our work focuses on the more realistic black-box attacks, where the attacker only has query-level access to the target. In this section, we describe prior work in two categories of attacks with black-box assumptions (substitute model attacks and query-based black-box attacks). We then describe five state-of-the-art (query-based) black-box attacks (including two variants), and the lone proposed defense [13].

### 2.1 Substitute Model Attacks

In a substitute model attack, an attacker generates a sequence of specific queries on the target DNN model to generate a substantial dataset capable of training a local *substitute model* that shares classification boundaries as the target. Then the attacker generates adversarial examples on the substitute model, i.e. a standard white-box attack, with the goal that these adversarial examples will transfer to the target DNN and cause misclassifications. The feasibility of this attack was first demonstrated for untargeted adversarial examples on small models (MNIST) [37,38], while the attack was shown to be much more difficult on targeted attacks and larger models [29].

In practice, substitute model attacks have two major shortcomings. First, success rates for these attackers are low and eclipsed by the more common, query-based black-box attacks. Second, there are effective defenses [26,49] against them. Kurakin et al. [26] has shown that an adversarially trained model is robust against these attacks and Tramer et al. [49] further improves the defense method using ensemble adversarial training.

Our work targets the more effective query-based black-box attacks. Blacklight is easily combined with existing defenses [49] to build robust defenses against substitute model attacks and query-based attacks (details in the appendix).

### 2.2 Query-Based Black-Box Attacks

The second and more effective type of black-box attacks are often referred to as query-based black-box attacks. In these attacks, attacker repeatedly sends queries to a target DNN

model, and uses the result to iteratively optimize each successive query, with the goal of ultimately converging on a successful adversarial example. While these attacks often require thousands of queries to generate a single adversarial example, they are extremely effective, and often achieve 100% attack success rates even against larger DNN models. In addition, recent work [17] shows that query-based attacks are feasible in the physical world, and pose a genuine threat to safety and mission critical applications.

Black box attacks can vary significantly in number of queries required, depending on how much information is given by the target model. Black box attacks can be divided into *score-based attacks* and *decision-based attacks*.

**Score-based attacks.** Score-based attacks require the target model to return the per-class probabilities or confidence scores for each input query. Chen et al. [12] proposes the first such attack by computing coordinate-wise numerical gradients of the target model at each pixel per step, with zeroth-order stochastic coordinate descent. The attack optimizes the loss function  $f(x) = \max\{\log[\mathbb{F}(x)]_{L_t} - \max_{i \neq L_t} \log[\mathbb{F}(x)]_i, -\kappa\}$  where  $\mathbb{F}(x)$  is the output probabilities of the target model for  $x$ ,  $L_t$  is the label for  $x$ , and  $\kappa \geq 0$  is a tuning parameter for attack transferability. The attacker sends out a sequence of carefully crafted inputs to the target model and uses the output returned by the model to estimate the gradient  $\frac{\partial f(x)}{\partial x}$ .

A number of improvements followed. [2] reduces computation time by grouping the pixels at random or using PCA; [22] reduces queries by computing the vector-wise gradient with random vectors; [23] further extends this approach to incorporate time-dependent priors. Finally, [34] proposes an alternative optimization method that avoids sensitivity to choice of hyperparameters by replacing gradient estimation.

**Decision-based attacks.** Decision-based attacks assume that the model returns the output label for each query and nothing more. [3] proposes a gradient estimation free technique where the attacker starts from a large adversarial perturbation and then seeks to iteratively reduce the perturbation while staying adversarial. [22] also considers decision-based attacks, and proposes a proxy for the softmax probability by using a discretized score. HSJA [10] further speeds up boundary attack by introducing gradient approximation.

### 2.3 State of the Art Attacks

To empirically test our proposed defense, we identify and implement 5 state-of-art black-box attacks (listed in Table 1). These represent all combinations of score-based vs. decision-based attacks, as well as attacks based on gradient estimation and those that do not rely on gradient estimation. These include both score- and decision-based variants of the NES attack [22], as well as the most recent and advanced black-box attack (HSJA [10]). We briefly describe each attack below.

	Gradient Estimation-based	Gradient Estimation-Free
Score-based	NES - Query Limit [22]	ECO [34]
Decision-based	NES - Label Only [22] HopSkipJumpAttack (HSJA) [10]	Boundary Attack [3]

Table 1: 5 representative black-box attacks used in this work.

**NES Attack (2 variants).** The NES Attack [22] allows for gradient estimation in far fewer queries than previous works by maximizing the expected value of  $f(x)$  under a search distribution  $\pi(\theta|x)$ . The attack uses the estimated gradient to perform a projected gradient descent update [32]. NES uses natural evolution strategies [51] to speed up the attack, and includes two variants: *NES query limit* for score-based target models, and *NES label-only* for decision-based models.

**Boundary Attack.** Boundary Attack [3] is the first decision-based attack, and uses a gradient estimation free method. It is initialized with a random sample from the target label. In each iterative step, the attacker reduces the distance between the perturbed image and the original input while ensuring the perturbed image is still classified to the target label. The attack iterates until the distance between the perturbed image and the original input is within the given budget.

**ECO Attack.** ECO Attack [34] replaces gradient estimation with an efficient discrete surrogate to the optimization problem. Also, the surrogate exploits the underlying problem structure for faster convergence.

**HSJA Attack.** HSJA is the most recently proposed black-box attack [10], and improves the Boundary Attack [3] by augmenting it with gradient approximation. It also initializes a perturbed image using an image from the target label, and then iteratively alters that image to reduce the distance between it and the original input. Each iteration of the attack includes two steps. The first step uses binary search to find a sample near the decision boundary between the perturbed image and the original input. The second step estimates the gradient and computes the step size to move towards the classification boundary. Iterating these two steps helps the attack converge much faster than the original Boundary Attack.

### 2.4 Existing Defense

We are only aware of one proposed defense against query-based black-box attacks, Stateful Detection (SD), in an arxiv paper by Chen, Carlini and Wager [13]. It augments an existing classifier with a detection component, which stores the similarity vectors for all incoming queries, computed by a pretrained similarity encoder, in a temporary history buffer. For each new query, it computes k-nearest-neighbor distance between it and all similarity vectors in the history buffer.

SD has two major limitations. First, due to the complexity of training a similarity encoder, SD is only implemented on small datasets like CIFAR-10 [13]. Second, due to the high cost of computing query similarity, SD also resets the detector after each detected attack query [13]. Later in §7.3,

we evaluate Blacklight against SD on CIFAR-10, and show that SD only detects a small proportion of all queries in an attack, making it vulnerable to a persistent attacker who issues multiple attack queries using multiple accounts.

### 3 Threat Model

We begin by defining our threat model.

**Attacker.** The *attacker* queries the target DNN model  $\mathbb{F}$  and uses the query results to craft adversarial examples against  $\mathbb{F}$ . Consider a targeted attack on misclassifying a source input  $x_0$  to a target label  $L_t$ . The attacker repeatedly queries  $\mathbb{F}$  with a sequence of  $n$  attack queries  $(x_0, x_1, \dots, x_n)$ , where  $x_n$  is the last query of the attack. The attack is successful if

$$\mathbb{F}(x_n) = L_t \quad \text{and} \quad \|x_n - x_0\|_p < \varepsilon \quad (1)$$

where  $\varepsilon$  is the attack perturbation budget. Existing works show that  $n$  is in the order of  $10^3$  to  $10^6$ .

We make the following assumptions on the attacker:

- The attacker does not have access to the internal weights of  $\mathbb{F}$  and can only send queries to obtain outputs of  $\mathbb{F}$ .
- The attacker has abundant computation power and resources to submit millions of queries.
- The attacker owns and controls a number of user accounts and IP addresses, which it uses to avoid IP address and account blocking. When banned, a persistent attacker simply continues its attack on a different IP address and/or account. Measurement studies show that it is common for attackers to utilize many *Sybil* accounts in online attacks [15, 28, 53]. SD [13] also considers attackers with multiple accounts.
- We initially consider standard attackers who are unaware of Blacklight. Later in §8, we consider stronger adaptive attackers who customize countermeasures in order to avoid our detection.

**Defender.** The *defender* hosts the target model  $\mathbb{F}$ . For each query,  $\mathbb{F}$  can either return the classification probability vector or just the classification label. We make the following assumptions on the defender:

- The defender has access to the queries submitted to  $\mathbb{F}$ , and a reasonable amount of computing resources.
- The defender has a finite amount of storage resources where it stores data on past queries. The defender periodically resets data on past queries, *e.g.* every 1 or 2 days. This reset frequency can be tuned as desired to further increase the time to perform any successful attack for persistent attackers with unlimited resources.

**Detection Metrics.** The defender’s ultimate goal is to ensure no adversarial examples are processed by its model as inputs. With that in mind, there are two main success metrics for black-box defenses.

- *Attack Detection Rate.* An effective defense must be able to detect the presence of an attack, where we define an attack to be a sequence of queries which are all contributing to

computing a single adversarial example. *Attack detection rate* is the ratio of all attacks detected sometime before it successfully generates an adversarial example.

- *Attack Query Coverage.* Persistent attackers can easily share partial progress results across IP addresses and accounts if they are detected and banned. Without knowledge of exact attack parameters, a defender cannot distinguish between queries building towards an attack and an actual attack with the computed adversarial example. *Query coverage* is the ratio of all queries in an attack that are detected as non-benign queries by the defender.

## 4 Blacklight Overview

We propose *Blacklight*, a system to detect and mitigate query-based black-box attacks against DNN models. Blacklight achieves this by exploiting a fundamental invariant of black-box attacks: to construct adversarial examples that resemble benign inputs, attackers must query the target DNN model with a large number of images, many of which are *highly similar* in the input space. Blacklight distinguishes attack queries from benign queries by searching for this invariant in a model’s stream of input queries.

To enable fast and scalable similarity computation across millions of queries, Blacklight computes for each query a *probabilistic fingerprint*, a set of bit strings generated by secure one-way hashes that represent randomized samples of the query. Computing a query’s fingerprint hashes requires only a single pass to read the input query. Given a query, searching a data store for similar queries (above a fingerprint match threshold) is done by counting maximum frequencies of occurrences in a set of hash table collisions, with average run time independent of queries in the data store.

In this section, we present the high-level concept behind Blacklight, starting from the invariant property of black-box attacks that drives our design, followed by an overview of the probabilistic fingerprinting system. Our design of Blacklight focuses on image classification tasks. We leave extension to domains such as speech recognition and NLP to future work.

### 4.1 Invariant Property of Black-box Attacks

We design Blacklight to exploit a fundamental invariant of query-based black-box attacks – because a successful black-box attack must satisfy the perturbation constraint defined by Eq. (1), the attacker *must* submit some (at least two) image queries separated by small differences in the input space. Since this level of similarity rarely exists between benign queries, it can be used to accurately detect the attack while incurring minimal false positives.

More specifically, to craft adversarial examples under the perturbation constraint, a black-box attacker iteratively perturbs a query image  $x_{i+1}$ , based on query results from the model on the previous images  $\{x_j\}_{j \leq i}$ . The specifics of the



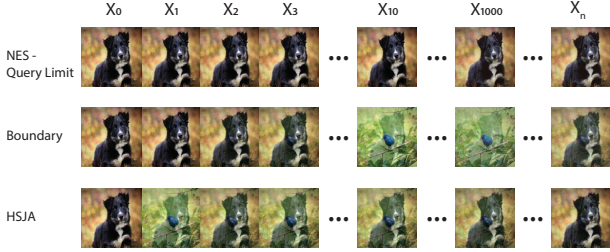


Figure 1: Examples of attack queries  $(x_0, x_1, x_2, \dots, x_n)$ , generated by 3 black-box attacks. Attacks produce a sequence of input queries starting with the original source image  $x_0$  and culminating in  $x_n$ , the final adversarial example. While attacks vary in how they search for adversarial examples, similar query images are common across all attack sequences.

iterative perturbations vary across algorithms: some start with the original input and perturbs it towards a misclassified target label [22, 34], while others start from an image in the target label and work backwards towards the original input [3, 10, 22]. In each case, the attacker seeks to repeatedly refine the perturbation between the original input and a potential adversarial example until it invariably converges on an adversarial example that is highly similar to the original input image in the input space. Mathematically, there exist attack queries  $\{x_i\}$  that

$$\min_{0 \leq j < i} \|x_i - x_j\|_p \leq \mu, \quad (2)$$

and  $\mu$  is a small number. If  $\mu$  is smaller than the difference between most benign queries, we can accurately recognize  $x_i$  as an attack image by comparing it to the queries stored in the defender database. As long as  $x_i$  is highly similar to any previous attack queries stored in the database, it will be detected by Blacklight. Evading this type of detection is extremely difficult (if not infeasible) since it requires each attack query  $x_i$  to be sufficiently dissimilar from *any* previous attack queries  $x_j$ ,  $0 \leq j < i$ . Clearly, this requirement contradicts with the attack perturbation constraint defined by Eq. (1).

In Figure 1, we demonstrate the invariant property using query images generated by launching 3 of the attacks summarized in §2 on *ImageNet* (we omit NES Label-only and ECO for brevity because they produce similar traces). We show a sample of images in the sequence of attack queries from the original  $x_0$  to the final adversarial example  $x_n$ . Similarity between images in a sequence are common, and average  $L_2$  distances between consecutive attack queries are a factor of 20-380x smaller than analogous distances between benign images (calculated by randomly choosing 2000 pairs of images from *ImageNet*).

## 4.2 Efficient Detection of Perturbed Images

Leveraging this invariant property of black-box attacks, one can now detect attack queries by searching for queries with high similarity in a large stream of incoming queries. A naive

approach would store all queries and compare an incoming query  $x$  to previous queries in the database and compute their  $L_p$  distances. This, however, is infeasible in practice because a model  $\mathbb{F}$  can receive a large set of queries per day, *e.g.* millions or tens of millions. Image-based query comparison requires intractable costs both in storage (to store raw query images) and in computational costs. For example, on the ImageNet dataset (224x224 pixels), it takes 23 minutes to compare a single query image and one million prior images, computed via five threads on a 6-core Intel Xeon server.

**Probabilistic Fingerprints.** Blacklight overcomes this challenge by applying a probabilistic algorithm that detects highly similar images.

One alternative would be to compute a hash signature per query image, using a distance-preserving hashing function, *e.g.* a locality-sensitive hash or locality-preserving hashing algorithm. However, locality-sensitive hashes lack the capacity to capture small differences in large files, locality-preserving hashes are easily reversed and manipulated to avoid detection by an adaptive adversary. Instead, what we want is a hash function that is compact, and yet highly sensitive to very small changes in the image. This dictates that we use a highly lossy function. The probabilistic fingerprints achieve these properties, and utilize secure one-way hashes that cannot be easily reversed to avoid detection.

We take all continuous segments of some fixed length  $w$  from the image, and apply a one-way hash to each segment to produce a large set of hash values. From these, we choose a small set (*e.g.* 50) of hash values, which together form the image’s probabilistic fingerprint. Figure 2 illustrates an example. For each incoming query  $x$ , Blacklight extracts its probabilistic fingerprint and stores it in the database. Blacklight then runs an efficient hash match algorithm to detect overlaps between  $x$ ’s fingerprint and previously stored fingerprints. Upon detecting sufficient overlap between  $x$  and an existing fingerprint  $y$ , Blacklight flags  $x$  and  $y$  as a pair of attack images. That is, using fingerprinting matching, Blacklight successfully identifies the two attack images “buried” in many benign images.

This fingerprint scheme has the property that any two highly similar query images will have near-perfect matches in their fingerprints. In other words, small changes to an image are highly unlikely to impact the image’s fingerprint. The secure one-way hash and downsampling of the hash values means that unless they can reverse the hashing algorithm, a clever adversary cannot significantly alter the fingerprint of an image without significantly altering the image itself.

In addition to dramatically reducing the storage overhead of past queries, Blacklight’s probabilistic fingerprints also significantly reduce the computation complexity of searching for similar queries. The search for similar queries reduces down to a hash collision counting problem, which takes near-constant time for the common case (see §5).

**Prior Work.** Probabilistic fingerprints have been used for

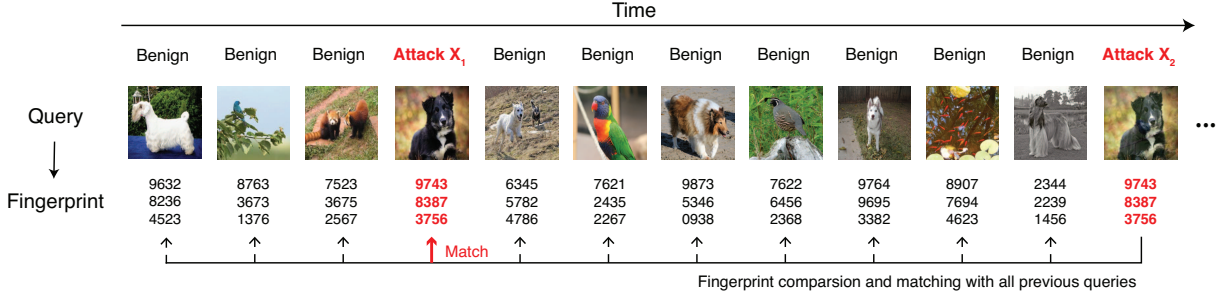


Figure 2: Blacklight computes for each raw image a small set of hash entries (a probabilistic fingerprint). Blacklight detects attack images hidden inside a large stream of benign images by comparing and detecting highly similar fingerprints.

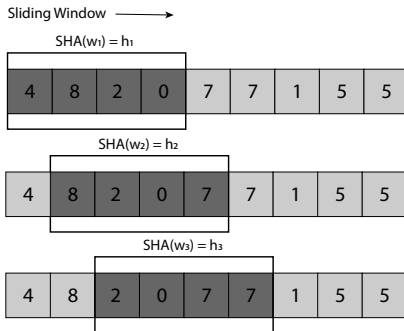


Figure 3: Computing content hashes w/ a sliding window.

similarity detection in the text domain, identifying source code plagiarism [4, 16, 42, 45], network intrusions and malware [36, 41, 46] and even spam emails [30, 57]. It was also used in *sif*, a similarity detector for file systems [33].

Our work extends probabilistic fingerprinting beyond the text domain and uses it to identify similar image queries submitted to a model. The continuous nature of images makes the similarity comparison difficult because a small value change on an input will change its fingerprint. We address this problem next in §5 with pixel quantization.

## 5 Detailed Design of Blacklight

We begin this section by presenting details of the Blacklight system and the details of the fingerprint generation process. We then describe scalability optimizations to further reduce computation and storage overheads, and enhancement to improve robustness. Finally, we discuss our thoughts on different approaches to mitigate attacks post-detection.

### 5.1 System Details

The goal of Blacklight is to protect a DNN model by computing for each incoming query image a small (fixed) set of hash entries, and then comparing this fingerprint to stored fingerprints of prior queries to determine if the new query has extremely high similarity to any prior query. Our hypothesis is that most images produced during a black-box attack share

high content similarity, and this invariant property is the key to Blacklight’s detection.

Blacklight achieves this goal in three steps.

**Step 1: Pixel Quantization.** Given an input query  $x$ , Blacklight first applies a quantization function to each pixel value of  $x$ . This has two purposes. First, quantization converts the continuous pixel value space into a finite set of discrete values, which are then used to compute hash values. Second, quantization also helps to increase the similarity between (attack) images, since some black-box attacks choose to modify every pixel with extremely small values. Quantization effectively nullifies the contribution of those minor modifications.

**Step 2: Computing fingerprints.** To produce the fingerprint on a (quantized) query image, Blacklight first “flattens” the 2-D image into a linear pixel sequence by combining rows of pixels together. The length of the vector is  $|x|$ , the total number of pixel elements of the input  $x$ . Blacklight then applies a sliding window of size  $w$  on this single vector, iteratively moving the sliding the window by  $p$  (referred to as the sliding step). This produces  $N = (|x| - w + p)/p$  fixed size vectors, each of length  $w$ . Any two subsequent vectors overlap by  $w - p$  entries, and each pixel in  $x$  is included in  $w/p$  consecutive vectors.

Next, Blacklight applies a secure one-way hash function (e.g. SHA-3 combined with a random salt value chosen by the defender) to each vector  $i$  ( $i \in [1, N]$ ), producing a hash entry  $h_i$  based on vector  $i$ ’s pixel values. This creates a full hash set  $\mathbf{H}_x = (h_1, h_2, \dots, h_N)$  for query  $x$ , which contains  $N$  hash entries. For example, for CIFAR10 where  $|x| = 32 \times 32 \times 3 = 3072$ , we have  $N = 3053$  when  $w = 20$ ,  $p = 1$ . An example of this sliding window hashing scheme is shown in Figure 3.

Finally, instead of using  $\mathbf{H}_x$  as  $x$ ’s fingerprint, Blacklight selects the top  $S$  hash values in  $\mathbf{H}_x$  (sorted by numerical order) as its probabilistic fingerprint (denoted as  $\mathcal{S}(\mathbf{H}_x)$ ). Since the output distribution of the one-way hash function should be highly random, choosing the top  $S$  subset by numerical sort serves as an efficient downsampling algorithm that is both deterministic (i.e. the same image will always produce the same set of  $S$  hash values), and unpredictable by an adversary (predicting the top  $S$  hash values in numeric order requires

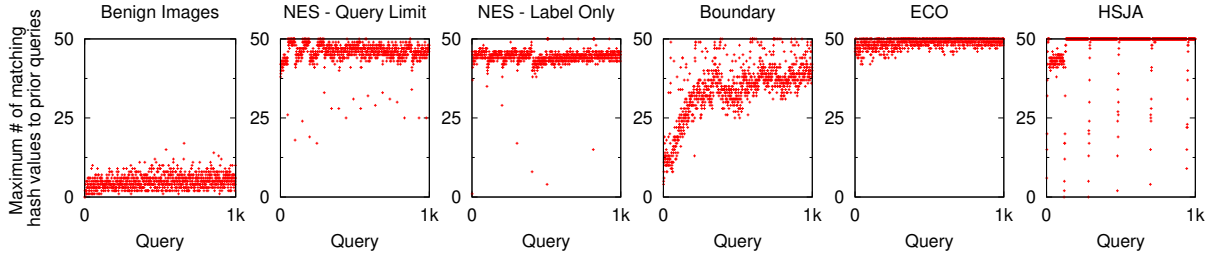


Figure 4: We empirically show that our proposed probabilistic fingerprints are able to identify the invariant property in black-box attack sequences. We plot the *maximum fingerprint overlap* between  $x$  and that of any prior query in the sequence. The fingerprint overlap between two queries  $x$  and  $y$  is defined by  $|\mathbb{S}(\mathbf{H}_x) \cap \mathbb{S}(\mathbf{H}_y)|$ . We plot this a sequence of 1000 randomly chosen benign queries, and for the first 1000 attack queries generated by five representative black-box attacks.

accurately predicting all hash values for all pixel vectors in an image).

We illustrate this property in Figure 4 by computing the similarity across query fingerprints  $\mathbb{S}(\mathbf{H}_x)$ . We consider a sequence of 1000 random benign image queries, and attack sequences generated by each of our 5 black-box attacks. For each query  $x$  in each sequence, we compute the *maximum* number of matching hash values between  $x$ 's fingerprint and that of any prior query:  $|\mathbb{S}(\mathbf{H}_x) \cap \mathbb{S}(\mathbf{H}_y)|$ . While each fingerprint only contains  $\mathbf{S} = 50$  hash entries, the disparity in results between benign sequences and attack sequences is obvious. Benign queries share minimal overlap with prior queries. In sequences generated by the five attacks, there exist many attack queries whose fingerprints are highly similar to at least one of previous attack queries, allowing Blacklight to detect the attack in its early stage.

**Step 3: Comparing and matching fingerprints.** Upon receiving a new query  $x$ , Blacklight will compute its fingerprint  $\mathbb{S}(\mathbf{H}_x)$  and compare it with all the fingerprints stored in the database. If any stored fingerprint shares more than  $\mathbf{T}$  hash entries with  $\mathbb{S}(\mathbf{H}_x)$ , then  $x$  is flagged as an attack image. Here the value of  $\mathbf{T}$  can be configured to meet the desired false positive rate. Later in §6, we analytically show that by properly configuring  $\mathbf{T}$  and  $\mathbf{S}$ , we can achieve accurate attack detection at a low false positive rate.

Computing the maximum overlap between the fingerprint of a query and  $m$  stored fingerprints is non-trivial. A simple algorithm would incur computation cost of  $O(m)$ . A slightly better algorithm can store a query  $x$ 's fingerprint into a hashmap using each of its hash entry as a key. The maximum overlap with all  $m$  queries can be found by retrieving all queries associated with each key in  $x$ 's fingerprints, and counting the max frequency of any query in that set. An efficient implementation can produce average runtime cost that is a constant independent of  $m$ . We leave the design and analysis of an efficient hashset matching algorithm to future work.

**Scalability.** In practice, the defender can periodically (*e.g.* once per day) reset the fingerprints of prior queries to avoid overflowing local storage (and also refresh the salt value for

the secure hash). An attacker can attempt to space its black-box queries across different days to evade detection, we consider this Pause and Resume attack in §8.1.

## 5.2 Attack Mitigation

The ultimate goal of a defense is to ensure no adversarial examples reach the protected DNN model. Detecting the presence of a black-box attack is insufficient, since a persistent attacker can simply switch accounts and/or IP addresses and continue where the previous query left off. Here, we discuss different options for mitigation after an attack is detected.

**Ban accounts.** A simple response to a detected attack query is to ban the account where it came from. Though easy to implement, this approach has two issues. First, this increases the penalty for a false positive, which might negatively impact wide deployment. Second, resource rich attackers can continue the attack using Sybil accounts, which are difficult to eradicate in practice.

**Return misguided outputs.** We also consider a more elaborate scheme where the defender intentionally misleads the attacker by returning carefully biased query outputs, perhaps towards secondary goals like identifying the attacker. This approach faces additional challenges. First, crafting biased responses requires significantly more computation and state-keeping at the defender. Second, the defender must be careful to avoid returning valid responses to actual attacks.

**Reject all detected queries.** We choose a simple mitigation strategy: reject all detected attack queries. This mitigation is effective in preventing attacks *IFF* the ratio of attack queries detected is high. If most attack queries are rejected, the attack sequence takes a very long time to converge and succeed. The benefit of this approach is that it does not rely on detecting or reducing Sybil accounts, and false positives have minimal impact on benign users. We further evaluate the impact of mitigation on persistent attackers in §7.

## 6 Formal Analysis of Blacklight

We perform a formal analysis on whether Blacklight can distinguish between benign and attack queries. Our analysis starts from a formal model on Blacklight’s probabilistic fingerprinting process, using which we run a detailed analysis on the probability of Blacklight flagging an image pair  $(x, y)$  as attack queries. We use this to compute Blacklight’s false positive rate and attack query detection rate, and examine their dependency on  $T$ , the fingerprint matching threshold.

**Definition 1. Hash Function** is a function that, for a given input  $x$ , produces  $N$  hash values,  $\mathbf{H}_x = (h_1, h_2, \dots, h_N)$ . Each entry  $h_i$  is a positive integer that is independent and identically distributed (I.I.D.) in the hash space  $[1, \Omega]$ , where  $\Omega$  is a very large positive integer,  $\Omega \gg N$ . Without loss of generality,  $h_i$  follows a uniform distribution within  $[1, \Omega]$ .

**Definition 2.** Given two queries  $x$  and  $y$ , we represent their full hash set as  $\mathbf{H}_x = \mathbf{H}_{sh} \cup \hat{\mathbf{H}}_x$  and  $\mathbf{H}_y = \mathbf{H}_{sh} \cup \hat{\mathbf{H}}_y$ , where  $\mathbf{H}_{sh} = \mathbf{H}_x \cap \mathbf{H}_y$ ,  $\hat{\mathbf{H}}_x \cap \hat{\mathbf{H}}_y = \emptyset$ ,  $|\mathbf{H}_{sh}| = N - D$ ,  $|\hat{\mathbf{H}}_x| = |\hat{\mathbf{H}}_y| = D$ . For simplicity, we assume  $\mathbf{H}_{sh} \cap \hat{\mathbf{H}}_x = \emptyset$ ,  $\mathbf{H}_{sh} \cap \hat{\mathbf{H}}_y = \emptyset$ .

The amount of hash difference  $D$  between  $x$  and  $y$  depends on whether  $(x, y)$  is a pair of benign inputs or attack inputs:

$$D = \begin{cases} \delta_{benign}, & (x, y) \text{ is a benign input pair} \\ \delta_{attack}, & (x, y) \text{ is an attack input pair} \end{cases}$$

where  $\delta_{attack}$  is a small number determined by the attack perturbation budget. In general we have  $\delta_{benign} \gg \delta_{attack}$ .

**Definition 3. Probabilistic Fingerprinting (PF)** is a function performed on the full hash set that samples top  $S$  hash entries out of  $\mathbf{H}_x$ , i.e.  $\mathbb{S}(\mathbf{H}_x) = (h'_1, h'_2, \dots, h'_S) \subset \mathbf{H}_x$ .

Blacklight operates on  $\mathbb{S}(\mathbf{H}_x)$  to detect attack queries rather than the full hash set  $\mathbf{H}_x$ . Blacklight marks  $(x, y)$  as attack images if  $|\mathbb{S}(\mathbf{H}_x) \cap \mathbb{S}(\mathbf{H}_y)| > T$ .

**Theorem 1.** Consider query pairs  $(x, y)$  whose full hash sets  $\mathbf{H}_x$  and  $\mathbf{H}_y$  differ by  $D$  entries (i.e.  $|\mathbf{H}_x \setminus \mathbf{H}_y| = D$ ). Let  $\mathbb{Q}(D) \triangleq \Pr(|\mathbb{S}(\mathbf{H}_x) \cap \mathbb{S}(\mathbf{H}_y)| > T)$  be the probability of Blacklight flagging any such  $(x, y)$  as attack images. Then  $\mathbb{Q}(D)$  is bounded:

$$\mathbb{Q}^-(D) \leq \mathbb{Q}(D) \leq \mathbb{Q}^+(D),$$

$$\text{where } \mathbb{Q}^+(D) \triangleq \sum_{k=T+1}^{\min(S, N-D)} \frac{\binom{N-D}{k} \cdot \binom{D}{S-k}}{\binom{N}{S}},$$

$$\mathbb{Q}^-(D) \triangleq \frac{\sum_{k=T+1}^{\min(S, N-D)} A_k}{\sum_{i=0}^{\min(S, N-D)} A_i}.$$

and  $A_i$  is defined in the appendix.

*Proof.* We prove the upper bound by considering a different PF function  $\mathbb{S}(\cdot)$  that selects  $S$  hash entries to maximize  $|\mathbb{S}(\mathbf{H}_x) \cap \mathbb{S}(\mathbf{H}_y)|$ . Similarly, we derive the lower bound by configuring a new PF to minimize  $|\mathbb{S}(\mathbf{H}_x) \cap \mathbb{S}(\mathbf{H}_y)|$  by independently selecting  $S$  entries from  $\mathbf{H}_x$  and  $\mathbf{H}_y$ . The detailed proof is listed in the appendix.  $\square$

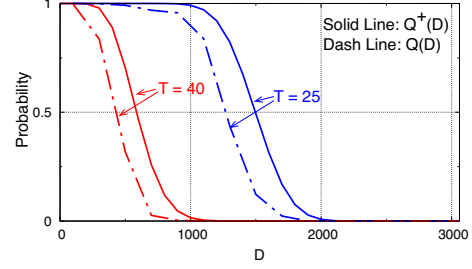


Figure 5: Comparing the theoretical upper bound  $\mathbb{Q}^+(D)$  and the actual  $\mathbb{Q}(D)$  derived from empirical experiments. The two metrics align with each other and both decay fast with  $D$ . The choice of  $T$  has a visible impact on both. Here  $S = 50$ ,  $N = 3053$  (CIFAR10),  $0 \leq D \leq N$ .

Figure 5 plots the numerical value of  $\mathbb{Q}^+(D)$  vs.  $D$ , for  $N = 3053$  (based on input size of CIFAR10,  $w = 20$ ,  $p = 1$ ),  $S = 50$  and  $T = 25$  or  $40$ . We see that  $\mathbb{Q}^+(D)$  decays very fast with  $D$ . We also empirically compute the actual  $\mathbb{Q}(D)$  vs.  $D$  curve by running Blacklight on both benign and attack queries generated using CIFAR10, under the same  $w$ ,  $p$ ,  $S$  and  $T$ . They are plotted as dashed lines in the same Figure. We see that our theoretical upper bound  $\mathbb{Q}^+(D)$  is a tight bound on  $\mathbb{Q}(D)$ . More importantly, both  $\mathbb{Q}^+(D)$  and  $\mathbb{Q}(D)$  decay very fast with  $D$ . The same applies to  $\mathbb{Q}^-(D)$ .

Using Theorem 1, we compute the false positive rate of Blacklight as the probability that two benign inputs are detected as attack inputs:  $P_{FP} = \mathbb{Q}(\delta_{benign})$ , and the attack query detection rate as  $P_{detect} = \mathbb{Q}(\delta_{attack})$ . Since  $\mathbb{Q}(D)$  decays fast with  $D$ , Blacklight should achieve  $P_{FP} \rightarrow 0$  and  $P_{detect} \rightarrow 1$  as long as  $\delta_{benign} \gg \delta_{attack}$ .

**Choosing  $T$ .** Given  $N$  and  $S$ , varying  $T$  will have a visible impact on  $\mathbb{Q}(D)$  – decreasing  $T$  could increase attack query detection rate at the cost of a higher false positive rate. One can examine the model’s training data to compute  $\delta_{benign}$  and use it to configure  $T$  to meet a desired false positive rate.

## 7 Experimental Evaluation of Blacklight

Using four different image classification tasks (and datasets), we now empirically evaluate Blacklight against five representative black-box attacks (as discussed in §2.3). Our experiments focus on understanding 1) the effectiveness of Blacklight in both attack detection and mitigation; 2) the improvement over existing defenses; and 3) Blacklight’s storage and computation overhead.

### 7.1 Experimental Setup

We apply Blacklight to defend against five representative black-box attacks (§2.3), using four different image classification tasks. These experiments involve DNN models  $\mathbb{F}$  with a wide range of input size/content and model architectures, allowing us to study Blacklight performance under a diverse



Task	Dataset	# Classes	Training data size	Test data size	Input size	Model architecture	Model accuracy
Digit Recognition ( <i>MNIST</i> )	MNIST	10	60,000	10,000	(28, 28, 1)	6 Conv + 3 Dense	99.36%
Traffic Sign Recognition ( <i>GTSRB</i> )	GTSRB	43	39,209	12,630	(48, 48, 3)	6 Conv + 3 Dense	97.59%
Object Recognition - Small ( <i>CIFAR10</i> )	CIFAR-10	10	50,000	10,000	(32, 32, 3)	ResNet20	91.48%
Object Recognition - Large ( <i>ImageNet</i> )	ImageNet	1000	1,281,167	50,000	(224, 224, 3)	ResNet152	73.05%

Table 2: Overview of classification tasks with their associated datasets and models.

set of conditions.

**Image Classification Tasks.** We consider four representative classification tasks, including *MNIST* [27], *GTSRB* [48], *CIFAR10* [24], and *ImageNet* [43]. We summarize key properties of each task and associated models in Table 2. The detailed information on model architectures and training configurations are in Table 13 in Appendix.

**Attack Configurations.** We implement and run the five black-box attacks against each of the above four classification models. For *MNIST*, *GTSRB* and *CIFAR10*, we randomly select 100 images from its test dataset and use each as the source image of the attack (*i.e.*  $x_0$ ). For *ImageNet*, we use 50 source images (due to its higher computation cost).

When configuring each attack, we follow its original paper and use the same L distance metric ( $L_2$  or  $L_\infty$ ) stated by the paper. We normalize the input value range to [0,1], and normalize  $L_2$  by the size of the input. We set the perturbation budget to 0.05 for all attacks and tasks. The only exceptions are  $L_\infty$  attacks against *MNIST* – we find that a perturbation budget of 0.1 is necessary for these attacks to succeed. The detailed attack parameters are listed in Table 3. Finally, we run each attack until it terminates (*i.e.* successfully generating an adversarial example) or until it reaches 100K queries, whichever occurs first.

**Blacklight Configuration.** Table 4 lists Blacklight’s default configuration of key parameters, including sliding window size  $w$ , sliding step  $p$ , quantization step  $q$ , number of hash entries per fingerprint ( $S$ ), and fingerprint matching threshold ( $T$ ). To show the generality of Blacklight, we set the parameters to be the same default values for all four tasks, rather than “optimizing” them for each task. The only exception is the sliding window size  $w$  – our default value is 20, but we increase it to 50 for *MNIST* (due to its large black background) and *ImageNet* (due to its large image size).

**Evaluation Metrics.** We use the following performance metrics to capture the effectiveness and cost of Blacklight.

- **False positive rate.**
- **Attack detection rate:** % of black-box attacks detected before the attack completes.
- **Detection coverage:** % of queries in an attack’s query sequence) identified as an attack query.
- **Average # of queries to detect:** Average number of attack queries received before Blacklight detects the attack.

	Attack Type	Attack detect %	Detection coverage	Queries to detect	Attack success	Median queries
<i>MNIST</i>	NES - QL	100%	99.4%	2	0%	DNF
	NES - LO	100%	98.9%	2	0%	DNF
	Boundary	100%	61.6%	19	0%	DNF
	ECO	100%	99.9%	2	0%	DNF
	HSJA	100%	98.3%	6	0%	7948
<i>GTSRB</i>	NES - QL	100%	98.7%	2	0%	24829
	NES - LO	100%	98.0%	3	0%	DNF
	Boundary	100%	64.0%	22	0%	DNF
	ECO	100%	100.0%	2	0%	2994
	HSJA	100%	98.3%	6	0%	3968
<i>CIFAR10</i>	NES - QL	100%	98.4%	2	0%	1961
	NES - LO	100%	98.4%	2	0%	6447
	Boundary	100%	68.8%	28	0%	2076
	ECO	100%	99.6%	2	0%	760
	HSJA	100%	96.4%	6	0%	957
<i>ImageNet</i>	NES - QL	100%	97.6%	3	0%	10213
	NES - LO	100%	95.2%	6	0%	DNF
	Boundary	100%	94.9%	48	0%	69509
	ECO	100%	99.9%	2	0%	3066
	HSJA	100%	98.3%	7	0%	12625

Table 5: Detection and mitigation results on all attacks and model combinations. *Attack success* represents success rate of attacks with Blacklight mitigation, and *Median queries* represents the median # of queries required to complete a specific attack. DNF denotes attacks where a median value was unavailable, because less than 50% of attacks finished in less than 100K queries.

- **Attack success rate with mitigation:** Success rate of a persistent attacker when Blacklight rejects all detected attack queries.
- **Detection overhead:** Run-time latency and storage costs.

**Setting Matching Threshold  $T$ .** Fingerprint matching threshold  $T$  is the key parameter that controls the tradeoff between detection rate and false positives. In practice, probabilistic fingerprints should perform well for a range of moderate values of  $T$ , e.g. threshold set to half of all hashes in the fingerprint ( $T \sim 0.5 \times S$ ). Figure 6 shows the false positive rates (across the entire test data) for different values of threshold  $T$ . We set  $T$  to a default value of 25 ( $0.5 \times S$ ), which achieves low false positives (<0.1%) and high detection for nearly all of our attacks.

## 7.2 Attack Detection and Mitigation

We evaluate Blacklight’s detection rate by implementing and performing each of the five black-box attacks against each classification model. For each attack and task combination,

Attack Type	Distance Metric	Perturbation Budget
NES - QL	$L_\infty$	0.05 (0.1 for <i>MNIST</i> )
NES - LO	$L_\infty$	0.05 (0.1 for <i>MNIST</i> )
Boundary	$L_2$	0.05
ECO	$L_\infty$	0.05 (0.1 for <i>MNIST</i> )
HSJA	$L_2$	0.05

Table 3: Black-box attack configurations.

Task	<i>MNIST</i>	<i>GTSRB</i>	<i>CIFAR10</i>	<i>ImageNet</i>
Quantization step ( $q$ )	50	50	50	50
Sliding window size ( $w$ )	50	20	20	50
Sliding step ( $p$ )	1	1	1	1
# of hashes per fingerprint ( $S$ )	50	50	50	50
Matching threshold ( $T$ )	25	25	25	25

Table 4: Default configuration of Blacklight.

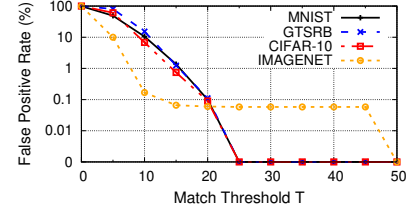


Figure 6: False positive rate for Blacklight’s attack detection under different choices of matching threshold  $T$  when  $S = 50$ .

we run 100 iterations of each attack (50 for *ImageNet*). Each attack iteration selects a random image from the test dataset as source image of the attack  $x_0$ , and a random incorrect label as the misclassification target label. Three attacks (NES - Label Only, Boundary and HSJA) require an image from the target label to perform the attack, and we select a random image belonging to the target label for that purpose.

The results for all attacks are listed in Table 5. First, we note that the attacks varied *significantly* on speed of convergence (# of queries before it produced an adversarial example  $x_n$ ). Many attacks failed to converge even after generating 100,000 queries. We performed additional tests, and for some attack types (particularly NES-Label Only and attacks on *MNIST*), increasing the query limit beyond 100K produced diminishing returns on attacks completed. In other words, the large majority of attacks that did not complete in 100K queries, still did not complete given 200K or 300K queries. To characterize the length of these attacks (many of which are unbounded), we show the median in numbers of queries to completion in the last column of Table 5 (Median Queries). We see that for most attacks, the median attack took between several hundred to tens of thousands of queries to complete.

We summarize key results from Blacklight’s detection. First, Blacklight detects all attacks on all models in progress (Attack detection rate is 100% for all tests). Second, detection coverage is extremely high: Blacklight detects more than 96% of all attack queries, except on the Boundary attack, whose algorithm converges to the adversarial example very slowly<sup>4</sup>. Third, Blacklight detect a new attack very quickly, often after a handful of (2–6) queries (again, more queries required for Boundary because it converges slower). In all cases, Blacklight detects an attack in less than 1% of the queries it takes for the median attack to complete.

When Blacklight rejects queries that it identifies as attack queries, 0% of persistent attackers manage to complete their attack within 100K attack queries. Blacklight’s mitigation is highly effective because it is able to detect a large majority of attack queries. By rejecting these queries, Blacklight prevents the attacker from making forward progress in probing model

<sup>4</sup>We note that Boundary and NES-LO take the longest time to converge. Less than 50% of NES-LO complete in 100K queries for *MNIST*, *GTSRB* and *ImageNet*.

Attack	Detection coverage	Avg queries to detect	Attack success w/ mitigation
NES - QL	1.8% / <b>98.4%</b>	52 / 2	97% / <b>0%</b>
NES - LO	1.3% / <b>98.4%</b>	52 / 2	85% / <b>0%</b>
Boundary	1.0% / <b>68.8%</b>	54 / <b>28</b>	82% / <b>0%</b>
ECO	1.8% / <b>99.6%</b>	53 / 2	78% / <b>0%</b>
HSJA	1.7% / <b>96.4%</b>	52 / 6	100% / <b>0%</b>

Table 6: Performance comparison between Stateful Detection and Blacklight on *CIFAR10*, in terms of attack detection and mitigation. The result is presented as “Stateful Detection / **Blacklight**” where the result of Blacklight is bold.

classification boundaries. As such, a high detection coverage is critical to defend against black-box attacks.

**Key Takeaways.** In summary, Blacklight detects all attacks on all models, detects the overwhelming majority of individual queries in the attack sequence, and detects the attack quickly (usually in less than 10 queries, with the exception of the slow converging Boundary attack). When Blacklight mitigation is active (it rejects queries identified as attacks), no attacks across our attack types and models are able to complete an attack in 100K queries.

### 7.3 Comparison with Prior Work

The only existing defense we know from literature is the Stateful Detection (SD) method from a 2019 arxiv report [13]. We compare Blacklight side-by-side against SD, using parameters specified in [13]. We can only provide experimental results on *CIFAR10*, because the authors of SD only shared their proposed similarity encoder for *CIFAR10*.

Table 6 compares the attack detection and mitigation performance between SD and **Blacklight** (results in **bold**). While both methods can detect the presence of the black-box attack (before it succeeds), Blacklight outperforms SD significantly in detection coverage. While SD can only detect a very small portion of the attack queries (less than 2%), Blacklight achieves 68+% coverage for Boundary and 96+% coverage for all other attacks (NES-QL, NES-LO, ECO, HSJA). As such, Blacklight can completely disable the attack by rejecting attack queries, reducing success rate of all instances of each attack type to 0% (after 100K queries). On the other

hand, since SD only detects (and responds to) a small percentage ( $< 2\%$ ) of attack queries, it has limited ability to slow down persistent attackers. Success rates of persistent attackers against SD range from 78% (ECO) to 100% (HSJA).

We believe SD’s low detection coverage is a consequence of the high computation complexity of its similarity detection algorithm. To scale to a large number of queries, SD resets its detector upon detecting an attack query. It assumes that banning the user account used to submit the attack query stops the attack. In practice, this assumption often fails because attackers can easily coordinate a single attack sequence across multiple accounts. In contrast, Blacklight’s more lightweight similarity computation allows it to compare each query against 100,000 prior fingerprints in a few milliseconds (Figure 7). We give more detailed performance analysis of Blacklight and SD in the next section.

## 7.4 Performance Overhead

Next, we take a closer look at runtime latency of Blacklight and SD, using measurements on an Intel i7 desktop server with 64 GB memory. Computing hash signatures is a fixed cost per image (and incurs negligible latency on today’s hardware), so the bulk of per-query costs come from searching for matching fingerprints in a large database of fingerprints of prior queries.

We measure Blacklight fingerprint matching latency for small ( $32 \times 32$ , *CIFAR10*) and larger ( $224 \times 224$ , *ImageNet*) images, using default configurations from Table 4. For different configurations, Figure 7 plots Blacklight’s latency to search for fingerprint matches (per incoming query) as a function of the number of queries stored in the database ( $n$ ). The curves are flat over  $n$ , suggesting that in the common case, Blacklight’s matching cost is near-constant and independent of  $n$ . In contrast, we also plot SD’s per-query match latency (only available for CIFAR) for different database sizes (no resets). It scales linearly with database size, and quickly surpasses Blacklight per-query latency for all but the smallest databases. Note that we can dramatically reduce per-query match time for Blacklight by increasing the sliding step  $p$  from 1 up to  $w/2$ . For larger images, this helps us avoid growth of total hashes per query, and has minimal impact on detection performance. We omit additional detailed performance tuning results due to space constraints.

Finally, hash-based fingerprints are extremely small in terms of storage costs. Across all parameters in our experiments, a fingerprint is at most  $32 \cdot S$  bytes (160B for our default configuration). Thus fingerprints for 1 million queries would only require 2GB of storage, a “negligible” value for modern servers.

## 8 Robustness Against Adaptive Attacks

Any meaningful defense must be robust against countermeasures from adaptive attackers with knowledge of the defense.

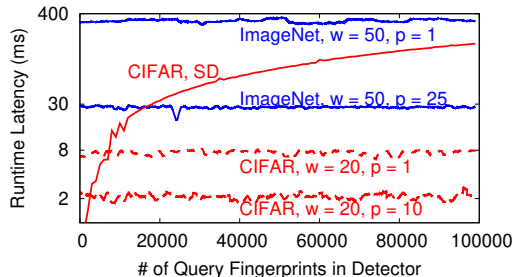


Figure 7: Blacklight’s runtime latency for *CIFAR10* and *ImageNet* as a function of the number of queries in the database. Note the log Y axis. Blacklight’s hashtable based matching algorithm produces latency that is independent of size of database for the common case. In contrast, SD’s algorithm is significantly slower and scales linearly with # of entries in the database. This forces SD to frequently reset their database, resulting in low detection coverage.

In this section, we consider two types of adaptive adversaries: *skilled adversaries* who know the target model is protected by Blacklight without specific knowledge of the detailed parameters, and *oracle adversaries*, who know everything about the Blacklight defense, including hashing window size, quantization values, etc. The only thing they do not have are the salt values added to the hash algorithms, since those are randomly generated every time the database resets.

We explore potential countermeasures in two broad categories. First, we consider attackers who try to evade Blacklight detection by modifying the attack. Second, we study Blacklight’s robustness against ideal attacks that go beyond the constraints for today’s attacks.

### 8.1 Evading Blacklight Detection

Blackbox attacks use iterative queries to estimate the loss surface around a source image. One possibility for evasion is to apply controlled noise to attack queries, in a way that does not disrupt classification, but may be significant enough to create significant differences in query fingerprints, and force Blacklight to overlook the similarity to prior queries. We propose 4 different adaptive attack strategies and evaluate the attack success rate and our attack detection rate over them.

**Perturbing Queries with Image Transformations (Skilled Adversary).** To magnify differences between attack queries, we can add additional perturbations to new queries. Here we explore 2 types of image transformation methods: adding noise and applying image augmentation. We *first* add different magnitudes of Gaussian noise to each attack query. *Second*, we apply different image augmentation like shift, rotation, zoom and blending to each attack query.

Table 7 shows that attack success rate and detection rate for all the transformations of different attacks on *CIFAR10*. Note that for each image transformation, we are showing detection rate on *successful attacks*. Blacklight’s detection of failed attacks drops slowly as noise levels increase. Since failed

Attack Type		Transformation Type	Gaussian Noise with Different Standard Deviation						Image Augmentation			
			0.0001	0.0005	0.001	0.005	0.01	0.05	Shift	Rotation	Zoom	Combined
NES - Query Limit	Attack Success Rate		85%	80%	60%	15%	0%	0%	100%	75%	80%	60%
	Detection of Successful Attacks		100%	100%	100%	100%	N/A	N/A	100%	100%	100%	100%
NES - Label Only	Attack Success Rate		25%	20%	15%	15%	0%	0%	100%	45%	70%	20%
	Detection of Successful Attacks		100%	100%	100%	100%	N/A	N/A	100%	100%	100%	100%
Boundary	Attack Success Rate		90%	90%	90%	85%	45%	0%	90%	90%	90%	90%
	Detection of Successful Attacks		100%	100%	100%	100%	100%	N/A	100%	100%	100%	100%
ECO	Attack Success Rate		85%	0%	0%	0%	0%	0%	0%	0%	0%	0%
	Detection of Successful Attacks		100%	N/A	N/A	N/A	N/A	N/A	N/A	N/A	N/A	N/A
HSJA	Attack Success Rate		95%	20%	10%	5%	5%	0%	0%	5%	10%	15%
	Detection of Successful Attacks		100%	100%	100%	100%	100%	N/A	N/A	100%	100%	100%

Table 7: Attack success rate and Blacklight detection of successful attacks as attackers add different image transformations.

attacks are not of interest, we omit them for brevity.

For each setting, we run 20 attack traces. For Gaussian noise, we add different standard deviations of the Gaussian noise to each image query from 0.0001 to 0.05 (all inputs are normalized to  $[0, 1]$ ). Sufficient noise can disrupt the image fingerprint and evade detection. However, higher levels of noise make attacks harder to converge. Table 7 shows that as noise levels increase, attack success rates drop quickly. But at all noise levels, Blacklight is able to detect all of the successful attacks. Thus Gaussian noise has no discernable impact on Blacklight’s attack detection.

For image augmentation, we test 4 different cases where the attacker shifts each query by at most 10%, rotates each query by at most 10°, zoom each query by at most 10% and where the attacker combines these three techniques together. Table 7 shows that while different attacks react differently to image augmentation techniques (some still produce successful attacks while others fail completely), Blacklight is able to detect all successful attack traces under different type of augmentations.

**Increasing Learning Rates (Skilled Adversary).** Other than adding external transformations to queries, the attacker can also try to evade detection by tweaking their learning rate parameter to increase the difference between each attack queries. Learning rate controls the difference between two adjacent queries when estimating the gradients. This does not apply to gradient estimation free attacks (Boundary and ECO attacks). We only explore different learning rate for NES-QL, NES-LO and HSJA attacks. For two variants of NES, we gradually increase learning rate more than 1000 fold. While the attack success rate drops to 0%, detection success rate remains 100%. For HSJA, we gradually grow learning rate up to a factor of  $10^6$ -fold, until changes in learning rate no longer impacts gradient estimation results. We observe that the attack success rate steadily drops (eventually to 15%), but detection rate maintains 100% throughout.

**Pause and Resume Attack (Oracle Adversary).** An attacker with full knowledge of a Blacklight system can exploit the fact that Blacklight periodically resets its database. An attacker can avoid detection by pausing their attack every time

Attack Type	Average Reset Cycles Needed	Average Total Queries
NES-QL	11471	12695
NES-LO	65837	67099
Boundary	2285	6160
ECO	5132	5133
HSJA	1092	1125

Table 8: Average reset cycles needed for a successful Pause and Resume attack on *CIFAR10*. The fastest attack (HSJA) can succeed in roughly 3 years.

it receives a rejection response, and resuming the attack the next time Blacklight resets its database. We run experiments through all 5 black-box attacks using this strategy against a *CIFAR10* model and Blacklight. We run 100 instances of each attack, and show average total queries needed for each attack to succeed, and the average number of reset cycles that requires in Table 8. If we reset Blacklight every 24 hours, the fastest successful attacker would complete an attack (using HSJA) in 1092 days or roughly 3 years. While this strategy does allow for a successful attack, the time cost to perform this attack is well beyond all but the most patient of attackers.

**Guided Image Transformation (Oracle Attacker).** Given perfect knowledge of Blacklight’s configuration values, an oracle attacker can compute precisely which pixels to modify so as to alter the maximum number of pixel vectors (and therefore maximum number of potential fingerprint hash values). A single post-quantization pixel change affects  $w/p - 1$  hash values. The perturbation must be large enough to survive quantization, and each query’s must choose its pixel perturbation to produce distinct hashes from that of all prior perturbations. We implement an oracle transformation algorithm that for each new query in the attack sequence, computes a minimum pixel perturbation that guarantees there are at most  $K$  hashes overlapping with prior query perturbations.

We apply two versions of this query perturbation scheme, where  $K = 0$  (all unique hashes) and  $K = T$  (expected to be barely detectable under threshold  $T$ ). Applying this to the two fastest converging attacks (HSJA and ECO), we find that the cumulative perturbations exceed the perturbation budget on



Attack Type	Default $T = 25$ (FPR = 0.0%)				$T = 15$ (FPR = 0.74%)			
	0.05	0.1	0.15	0.2	0.05	0.1	0.15	0.2
NES - QL	100%	100%	100%	100%	100%	100%	100%	100%
NES - LO	100%	100%	100%	100%	100%	100%	100%	100%
Boundary	100%	100%	75%	40%	100%	100%	100%	95%
ECO	100%	100%	100%	100%	100%	100%	100%	100%
HSJA	100%	100%	55%	40%	100%	100%	70%	40%

Table 9: Blacklight detection rate for attacks using larger perturbation budgets for *CIFAR10*. Lowering  $T$  dramatically improves detection even when allowing very large perturbations, with a small increase in false positives (0.74%).

*CIFAR10* after 23 queries ( $K = 0$ ) and 533 queries ( $K = T$ ). The takeaway is that while this attack provides successful evasion, the noise required quickly exceeds the entire attack perturbation budget, making it impractical.

## 8.2 Robustness against ideal attacks

Novel black-box attacks are being proposed at a rapid rate. Many of them break current assumptions on what black-box attacks can and cannot do. For example, future attacks may allow larger perturbation budgets, or find novel methods to dramatically reduce the number of queries necessary to converge to an adversarial example. In this section, we hypothesize about potential future black-box attacks that break current constraints, and evaluate Blacklight against some *ideal* black-box attacks.

**Increasing Attack Perturbation Budget.** Till now, our evaluation assumes attackers’ perturbation budgets are limited to commonly accepted values:  $L_{inf}/L_2 = 0.05$ . We hypothesize that future attacks might be able to tolerate a higher perturbation budget in specific attack domains or settings. Thus, we evaluate Blacklight’s detection performance against attacks on *CIFAR10* with perturbation budget.

For all attacks, we incrementally increase the perturbation from 0.05 all the way up to 0.2, and show Blacklight detection rate for each perturbation level (running 20 attack traces for each data point). We show that detection rates for NES variants and ECO continue steady at 100%, but Boundary and its related variant HSJA begin to evade detection at 0.15 and higher. To adapt, we try tuning fingerprint matching threshold  $T$ . We show in Table 9 that just by lowering  $T$  from 25 to 15, we can dramatically increase detection rates, restoring perfect detection to most attacks (except HSJA at 0.15 and 0.2 perturbation and Boundary at 0.2). This drop in  $T$  only increases false positive rates by 0.74%.

**Near-Optimal Black-Box Attacks.** Researchers are continually optimizing black-box attacks in terms of query efficiency. We consider it critical for Blacklight to resist more efficient attacks that are inevitable in the near future. Here we simulate Blacklight’s expected detection performance against two types of “near-optimal” black-box attacks. First, we consider extremely “query-efficient” black-box attacks that require several orders of magnitude fewer attack queries than

Attack Type	$N$			
	500	100	50	10
NES - Query Limit	100%	100%	100%	95%
NES - Label Only	100%	100%	100%	31%
Boundary	100%	90%	89%	48%
ECO	100%	100%	100%	100%
HSJA	100%	100%	100%	91%
CW	Average $N = 6.33$ , Detection rate = 100%			
PGD	Average $N = 3.13$ , Detection rate = 81%			

Table 10: Blacklight’s performance against near-optimal “query-efficient” and “perfect-gradient” black-box attacks.

current attacks. Second, we consider “perfect-gradient” black-box attacks who are able to estimate gradients as accurately as a white-box attack, and use white-box algorithms to guide their computation of adversarial examples.

To simulate Blacklight’s performance against a near-optimal query-efficient black-box attack, we evenly downsample attack query traces from our current 5 black-box attacks to generate attack traces that are a tiny fraction of current traces. We then test Blacklight’s detection performance on these subsampled attack traces. We show our results in Table 10. Even when our attacks are able to complete in 500, 100, or 50 queries, Blacklight can still detect them near perfectly (100% detection for 4 attacks and 89% for Boundary attack). Even when these attacks complete within 10 queries, Blacklight is still highly successful at detecting NES-QL, ECO and HSJA.

Finally, we imagine a perfect-gradient black-box algorithm that is somehow able to perfectly predict gradient functions from the results of its attack queries. Such an attack would converge on an adversarial example as quickly as a white-box algorithm that has full access to the full model. Each iteration of the gradient calculation for an analogous white-box attack would translate to a single query by the black-box attacker. The perfect gradient black-box attack applies attack algorithms such as CW [9] and PGD [32] to generate attack sequences against our *CIFAR10* model. On average, CW and PGD converge after only 6.3 and 3.1 queries. Against simulated black-box attacks using these attack queries, Blacklight detects 100% of attacks driven by CW, and 81% of PGD-driven attacks.

## 9 Conclusion

In this work, we present Blacklight, one of the first proposals to defend DNN models against query-based black-box attacks. It leverages the fundamental invariant of query-based black-box attacks: attackers must iteratively query the target model with a large number of similar images. Blacklight uses probabilistic fingerprints to scalably identify highly-similar image queries. Blacklight achieves near-perfect detection against a suite of state-of-the-art black-box attacks, with negligible false positives, and is robust to a range of adaptive and idealized countermeasures.

## References

- [1] ATHALYE, A., CARLINI, N., AND WAGNER, D. Obfuscated gradients give a false sense of security: Circumventing defenses to adversarial examples. In *Proc. of ICML* (2018).
- [2] BHAGOJI, A. N., HE, W., LI, B., AND SONG, D. Practical black-box attacks on deep neural networks using efficient query mechanisms. In *Proc. of ECCV* (2018).
- [3] BREDEL, W., RAUBER, J., AND BETHGE, M. Decision-based adversarial attacks: Reliable attacks against black-box machine learning models. In *Proc. of ICLR* (2018).
- [4] BRIN, S., DAVIS, J., AND GARCIA-MOLINA, H. Copy detection mechanisms for digital documents. In *Proc. of SIGMOD* (1995), pp. 398–409.
- [5] BUCKMAN, J., ROY, A., RAFFEL, C., AND GOODFELLOW, I. Thermometer encoding: One hot way to resist adversarial examples. In *Proc. of ICLR* (2018).
- [6] CARLINI, N., AND WAGNER, D. Defensive distillation is not robust to adversarial examples. *arXiv preprint arXiv:1607.04311* (2016).
- [7] CARLINI, N., AND WAGNER, D. Adversarial examples are not easily detected: Bypassing ten detection methods. *Proc. of AISec* (2017).
- [8] CARLINI, N., AND WAGNER, D. Magnet and efficient defenses against adversarial attacks are not robust to adversarial examples. *arXiv preprint arXiv:1711.08478* (2017).
- [9] CARLINI, N., AND WAGNER, D. Towards evaluating the robustness of neural networks. In *Proc. of IEEE S&P* (2017).
- [10] CHEN, J., JORDAN, M. I., AND WAINWRIGHT, M. J. Hopskipjumpattack: A query-efficient decision-based attack. In *Proc. of IEEE S&P* (2020), pp. 668–685.
- [11] CHEN, P.-Y., SHARMA, Y., ZHANG, H., YI, J., AND HSIEH, C.-J. Ead: elastic-net attacks to deep neural networks via adversarial examples. In *Proc. of AAAI* (2018).
- [12] CHEN, P.-Y., ZHANG, H., SHARMA, Y., YI, J., AND HSIEH, C.-J. Zoo: Zeroth order optimization based black-box attacks to deep neural networks without training substitute models. In *Proc. of AISec* (2017), pp. 15–26.
- [13] CHEN, S., CARLINI, N., AND WAGNER, D. Stateful detection of black-box adversarial attacks. *arXiv preprint arXiv:1907.05587* (2019).
- [14] DHILLON, G. S., AZIZZADENESHELI, K., BERNSTEIN, J. D., KOSSAIFI, J., KHANNA, A., LIPTON, Z. C., AND ANANDKUMAR, A. Stochastic activation pruning for robust adversarial defense. In *Proc. of ICLR* (2018).
- [15] DOUCEUR, J. R. The Sybil attack.
- [16] DUCASSE, S., RIEGER, M., AND DEMEYER, S. A language independent approach for detecting duplicated code. In *Proc. of ICSM* (1999), pp. 109–118.
- [17] FENG, R., CHEN, J., MANOHAR, N., FERNANDES, E., JHA, S., AND PRAKASH, A. Query-efficient physical hard-label attacks on deep learning visual classification. *arXiv preprint arXiv:2002.07088* (2020).
- [18] GOODFELLOW, I. J., SHLENS, J., AND SZEGEDY, C. Explaining and harnessing adversarial examples. *arXiv preprint arXiv:1412.6572* (2014).
- [19] HE, K., ZHANG, X., REN, S., AND SUN, J. Deep residual learning for image recognition. In *Proc. of CVPR* (2016), pp. 770–778.
- [20] HE, K., ZHANG, X., REN, S., AND SUN, J. Identity mappings in deep residual networks. In *European conference on computer vision* (2016), Springer, pp. 630–645.
- [21] HE, W., WEI, J., CHEN, X., CARLINI, N., AND SONG, D. Adversarial example defenses: Ensembles of weak defenses are not strong. In *Proc. of WOOT* (2017).
- [22] ILYAS, A., ENGSTROM, L., ATHALYE, A., AND LIN, J. Black-box adversarial attacks with limited queries and information. In *Proc. of ICML* (2018).
- [23] ILYAS, A., ENGSTROM, L., AND MADRY, A. Prior convictions: Black-box adversarial attacks with bandits and priors. In *Proc. of ICLR* (2019).
- [24] KRIZHEVSKY, A., ET AL. Learning multiple layers of features from tiny images. Tech. rep., Citeseer, 2009.
- [25] KURAKIN, A., GOODFELLOW, I., AND BENGIO, S. Adversarial examples in the physical world. *arXiv preprint arXiv:1607.02533* (2016).
- [26] KURAKIN, A., GOODFELLOW, I., AND BENGIO, S. Adversarial machine learning at scale. *Proc. of ICLR* (2017).
- [27] LECUN, Y., BOTTOU, L., BENGIO, Y., HAFFNER, P., ET AL. Gradient-based learning applied to document recognition. *Proc. of the IEEE* 86, 11 (1998), 2278–2324.
- [28] LEE, N. Having multiple online identities is more normal than you think. Engadget, March 2016. <https://www.engadget.com/2016/03/04/multiple-online-identities>.
- [29] LIU, Y., CHEN, X., LIU, C., AND SONG, D. Delving into transferable adversarial examples and black-box attacks. In *Proc. of ICLR* (2017).
- [30] LIU, Z., LIN, W., LI, N., AND LEE, D. Detecting and filtering instant messaging spam—a global and personalized approach. In *Proc. of ICNP NPSec Workshop* (2005).
- [31] MA, X., LI, B., WANG, Y., ERFANI, S. M., WIJEWICKREMA, S., SCHOENEBECK, G., SONG, D., HOULE, M. E., AND BAILEY, J. Characterizing adversarial subspaces using local intrinsic dimensionality. In *Proc. of ICLR* (2018).
- [32] MADRY, A., MAKELOV, A., SCHMIDT, L., TSIPRAS, D., AND VLADU, A. Towards deep learning models resistant to adversarial attacks. *arXiv preprint arXiv:1706.06083* (2017).
- [33] MANBER, U. Finding similar files in a large file system. In *Proc. of USENIX Winter Technical Conference* (1994), vol. 94, pp. 1–10.
- [34] MOON, S., AN, G., AND SONG, H. O. Parsimonious black-box adversarial attacks via efficient combinatorial optimization. In *Proc. of ICML* (2019).
- [35] MOOSAVI-DEZFOOLI, S.-M., FAWZI, A., AND FROSSARD, P. Deepfool: a simple and accurate method to fool deep neural networks. In *Proc. of CVPR* (2016).
- [36] OPRİŞA, C., CABĂU, G., AND PAL, G. S. Malware clustering using suffix trees. *Journal of Computer Virology and Hacking Techniques* 12, 1 (2016), 1–10.
- [37] PAPERNOT, N., MCDANIEL, P., AND GOODFELLOW, I. Transferability in machine learning: from phenomena to black-box attacks using adversarial samples. *arXiv preprint arXiv:1605.07277* (2016).
- [38] PAPERNOT, N., MCDANIEL, P., GOODFELLOW, I., JHA, S., CELIK, Z. B., AND SWAMI, A. Practical black-box attacks against machine learning. In *Proc. of ACM AsiaCCS* (2017).
- [39] PAPERNOT, N., MCDANIEL, P., JHA, S., FREDRIKSON, M., CELIK, Z. B., AND SWAMI, A. The limitations of deep learning in adversarial settings. In *Proc. of IEEE EuroS&P* (2016).
- [40] PAPERNOT, N., MCDANIEL, P., WU, X., JHA, S., AND SWAMI, A. Distillation as a defense to adversarial perturbations against deep neural networks. In *Proc. of IEEE S&P* (2016).
- [41] ROUSSEV, V. Hashing and data fingerprinting in digital forensics. *IEEE Security & Privacy* 7, 2 (2009), 49–55.
- [42] ROY, C. K., CORDY, J. R., AND KOSCHKE, R. Comparison and evaluation of code clone detection techniques and tools: A qualitative approach. *Science of computer programming* 74, 7 (2009), 470–495.
- [43] RUSSAKOVSKY, O., DENG, J., SU, H., KRAUSE, J., SATHEESH, S., MA, S., HUANG, Z., KARPATY, A., KHOSLA, A., BERNSTEIN, M., BERG, A. C., AND LI, F.-F. ImageNet Large Scale Visual Recognition Challenge. *International Journal of Computer Vision (IJCV)* 115, 3 (2015), 211–252.

- [44] SAMANGOUEI, P., KABKAB, M., AND CHELLAPPA, R. Defensegan: Protecting classifiers against adversarial attacks using generative models. In *Proc. of ICLR* (2018).
- [45] SHIVAKUMAR, N., AND GARCIA-MOLINA, H. Scam: A copy detection mechanism for digital documents. In *Proc. of ACM DL* (1995).
- [46] SINGH, S., ESTAN, C., VARGHESE, G., AND SAVAGE, S. Automated worm fingerprinting. In *Proc. of OSDI* (2004).
- [47] SONG, Y., KIM, T., NOWOZIN, S., ERMON, S., AND KUSHMAN, N. Pixeldefend: Leveraging generative models to understand and defend against adversarial examples. In *Proc. of ICLR* (2018).
- [48] STALLKAMP, J., SCHLIPSING, M., SALMEN, J., AND IGEL, C. Man vs. computer: Benchmarking machine learning algorithms for traffic sign recognition. *Neural Networks* (2012).
- [49] TRAMÈR, F., KURAKIN, A., PAPERNOT, N., GOODFELLOW, I., BONEH, D., AND MCDANIEL, P. D. Ensemble adversarial training: Attacks and defenses. In *Proc. of ICLR* (2018).
- [50] UESATO, J., O'DONOGHUE, B., OORD, A. V. D., AND KOHLI, P. Adversarial risk and the dangers of evaluating against weak attacks. *arXiv preprint arXiv:1802.05666* (2018).
- [51] WIERSTRA, D., SCHAUL, T., PETERS, J., AND SCHMIDHUBER, J. Natural evolution strategies. In *Proc. of IEEE World Congress on Computational Intelligence* (2008), pp. 3381–3387.
- [52] XIE, C., WANG, J., ZHANG, Z., REN, Z., AND YUILLE, A. Mitigating adversarial effects through randomization. In *Proc. of ICLR* (2018).
- [53] YANG, Z., WILSON, C., WANG, X., GAO, T., ZHAO, B. Y., AND DAI, Y. Uncovering social network sybils in the wild. *ACM Transactions on Knowledge Discovery from Data (TKDD)* 8, 1 (2014), 1–29.
- [54] YAO, Y., XIAO, Z., WANG, B., VISWANATH, B., ZHENG, H., AND ZHAO, B. Y. Complexity vs. performance: Empirical analysis of machine learning as a service. In *Proc. of IMC* (Nov. 2017).
- [55] ZANTEDESCHI, V., NICOLAE, M.-I., AND RAWAT, A. Efficient defenses against adversarial attacks. In *Proc. of AISec* (2017).
- [56] ZHENG, S., SONG, Y., LEUNG, T., AND GOODFELLOW, I. Improving the robustness of deep neural networks via stability training. In *Proc. of CVPR* (2016).
- [57] ZHOU, F., ZHUANG, L., ZHAO, B. Y., HUANG, L., JOSEPH, A. D., AND KUBIATOWICZ, J. Approximate object location and spam filtering on peer-to-peer systems. In *Proc. of ACM Middleware* (2003).

## A Detailed Proof for Theorem 1

We prove the upper and lower bounds separately below.

**Proof of Upper Bound.** Clearly  $\mathbb{S}(\mathbf{H}_x) = \mathbb{S}(\mathbf{H}_{sh} \cup \hat{\mathbf{H}}_x)$  will contain entries from  $\mathbf{H}_{sh}$  and  $\hat{\mathbf{H}}_x$ . The same applies to  $\mathbb{S}(\mathbf{H}_y)$ . Since  $\hat{\mathbf{H}}_x \cap \hat{\mathbf{H}}_y = \emptyset$ , the overlapping entries of  $\mathbb{S}(\mathbf{H}_x)$  and  $\mathbb{S}(\mathbf{H}_y)$  will only come from  $\mathbf{H}_{sh}$ . That is,

$$(\mathbb{S}(\mathbf{H}_x) \cap \mathbb{S}(\mathbf{H}_y)) \subset \mathbf{H}_{sh}, \quad (3)$$

$$(\mathbb{S}(\mathbf{H}_x) \setminus \mathbb{S}(\mathbf{H}_y)) \subset \hat{\mathbf{H}}_x \quad (4)$$

$$(\mathbb{S}(\mathbf{H}_y) \setminus \mathbb{S}(\mathbf{H}_x)) \subset \hat{\mathbf{H}}_y \quad (5)$$

To calculate the upper bound on  $Pr(|\mathbb{S}(\mathbf{H}_x) \cap \mathbb{S}(\mathbf{H}_y)| > T)$ , we consider the ‘‘optimal scenario’’ using a custom-designed<sup>5</sup> probabilistic fingerprinting process. When picking entries from  $\mathbf{H}_x$  and  $\mathbf{H}_y$ , the chosen entries in  $\mathbf{H}_{sh}$  are always the same for  $x$  and  $y$ . This is to maximize the similarity between  $\mathbb{S}(\mathbf{H}_x)$  and  $\mathbb{S}(\mathbf{H}_y)$ , which will be higher than that offered by selecting top  $S$  entries. Thus we compute  $\mathbb{Q}^+(D)$  as the probability of more than  $T$  entries in  $\mathbb{S}(\mathbf{H}_x)$  (and  $\mathbb{S}(\mathbf{H}_y)$ ) come from  $\mathbf{H}_{sh}$  and the rest come from  $\hat{\mathbf{H}}_x$  ( $\hat{\mathbf{H}}_y$ ). Since each hash entry’s value is IID, and  $|\mathbf{H}_{sh}| = N - D$ ,  $|\hat{\mathbf{H}}_x| = D$ , we calculate the probability following the hypergeometric distribution and arrive at  $\mathbb{Q}^+(D)$ .

**Proof of Lower Bound.** Following the above discussion, we derive the lower bound on  $\mathbb{Q}(D)$  by considering a ‘‘worst’’ case scenario: the probabilistic fingerprinting process picks  $S$  entries out of  $\mathbf{H}_x$  and  $\mathbf{H}_y$  fully independently, thus minimizing the similarity between  $\mathbb{S}(\mathbf{H}_x)$  and  $\mathbb{S}(\mathbf{H}_y)$ .

With this in mind, we compute a lower bound  $\mathbb{Q}^-(D)$  as the probability when the above fingerprinting process, when *independently* selecting entries from  $\mathbf{H}_x$  and  $\mathbf{H}_y$ , chooses more than  $T$  overlapping entries from  $\mathbf{H}_{sh}$  (again assuming hash entries are IID, thus each entry has the same probability of getting chosen):

$$\mathbb{Q}^-(D) = \frac{\sum_{k=T+1}^{\min(S, N-D)} A_k}{\sum_{i=0}^{\min(S, N-D)} A_i} \quad (6)$$

where  $A_i = \binom{D}{S-i} \binom{N-D}{i} \left( \binom{D}{S-i} + 2 \sum_{t=i+1}^{\min(S, N-D)} \binom{N-D-i}{t-i} \binom{D}{S-i} \right)$ . Here  $A_i$  computes the the number of cases where the two fingerprinting instances (one on  $\mathbf{H}_x$  and one on  $\mathbf{H}_y$ ) choose  $i$  overlapping entries from  $\mathbf{H}_{sh}$ .

## B Hybrid Defense against the Substitute Model Attack

Blacklight is designed to detect query based black-box attacks. It cannot defend against attacks transferred from a substitute

<sup>5</sup> One possible design is picking hash entries by their indices. If the fingerprinting process chooses the same set of hash indices for  $x$  and  $y$ , the chosen entries in  $\mathbf{H}_{sh}$  will be the same for  $x$  and  $y$ .

model. As we discussed in §2, substitute model attacks can be effectively stalled by an existing defense called ensemble adversarial training (EAT) [49]. EAT adversarially trains an ensemble of models with different architectures [32], which are shown to be robust against the substitute model attack. Hence, to defend against all types of black-box attacks, the defender can combine Blacklight with EAT to build a hybrid defense system.

We build and evaluate a hybrid Blacklight and EAT defense on the cifar task. Specifically, we build an ensemble model with three different architectures (6-layer CNN, 8-layer CNN, ResNet-20) and adversarially train the network using PGD attacks as suggested by [32]. We use the same Blacklight configuration as before.

We perform both substitute model based attacks and query based black-box attacks against the above ensemble model defended by Blacklight. For the substitute model attack we run the state-of-art attack proposed by Papernot et al [38], and for the query-based attacks we run the same five black-box attacks. The result shows that the hybrid defense works well and the two defenses do not interfere with each other. The substitute model attack achieves 0% success (thanks to EAT), and Blacklight achieves the same accurate attack query detection as reported before. Thus, we conclude that Blacklight, when combined with EAT, can defend against today’s black-box attacks.

## C Experiment Configuration

**Model Architecture.** We now present the architecture of DNN models used in our work.

- **MNIST** (Table 11) is a convolutional neural network (CNN) consisting of two pairs of convolutional layers connected by max pooling layers, followed by two fully connected layers.
- **GTSRB** (Table 12) is a CNN consisting of three pairs of convolutional layers connected by max pooling layers, followed by two fully connected layers.
- **CIFAR10** is a ResNet-20 [20] that includes 20 sequential convolutional layers, followed by pooling, dropout, and fully connected layers.
- **ImageNet** is the ResNet-152 [19] model trained on the ImageNet dataset [43]. It has 152 residual blocks with over 60 millions parameters.



Layer Index	Layer Name	Layer Type	# of Channels	Filter Size	Activation	Connected to
1	conv_1	Conv	32	3×3	ReLU	
2	conv_2	Conv	32	3×3	ReLU	conv_1
2	pool_1	MaxPool	32	2×2	-	conv_2
3	conv_3	Conv	64	3×3	ReLU	pool_1
4	conv_4	Conv	64	3×3	ReLU	conv_3
4	pool_2	MaxPool	64	2×2	-	conv_4
5	conv_5	Conv	128	3×3	ReLU	pool_2
6	conv_6	Conv	128	3×3	ReLU	conv_5
6	pool_3	MaxPool	128	2×2	-	conv_6
7	fc_1	FC	512	-	ReLU	pool_3
8	fc_2	FC	512	-	ReLU	fc_1
8	fc_3	FC	10	-	Softmax	fc_2

Table 11: Model Architecture for *MNIST*.

Layer Index	Layer Name	Layer Type	# of Channels	Filter Size	Activation	Connected to
1	conv_1	Conv	32	3×3	ReLU	
2	conv_2	Conv	32	3×3	ReLU	conv_1
2	pool_1	MaxPool	32	2×2	-	conv_2
3	conv_3	Conv	64	3×3	ReLU	pool_1
4	conv_4	Conv	64	3×3	ReLU	conv_3
4	pool_2	MaxPool	64	2×2	-	conv_4
5	conv_5	Conv	128	3×3	ReLU	pool_2
6	conv_6	Conv	128	3×3	ReLU	conv_5
6	pool_3	MaxPool	128	2×2	-	conv_6
7	fc_1	FC	512	-	ReLU	pool_3
8	fc_2	FC	512	-	ReLU	fc_1
8	fc_3	FC	43	-	Softmax	fc_2

Table 12: Model Architecture for *GTSRB*.

Table 13: Detailed information on datasets and defense configurations for each model dataset.

Model	Training Configuration
<i>MNIST</i>	epochs=50, batch=128, optimizer=Adam, lr=0.001
<i>GTSRB</i>	epochs=50, batch=128, optimizer=Adam, lr=0.001
<i>CIFAR10</i>	epochs=200, batch=32, optimizer=Adam, lr=0.001 (the learning rate is scheduled to be reduced after 80, 120, 160, 180 epochs)
<i>ImageNet</i>	Model trained and shared by He <i>et al.</i> [19]